

Evidence for multi-band strongly coupled superconductivity in $\text{SmFeAsO}_{0.8}\text{F}_{0.2}$ single crystals by high-field vortex torque magnetometry

L. Balicas,¹ A. Gurevich,¹ Y. J. Jo,¹ J. Jaroszynski,¹ D. C. Larbalestier,¹ R. H. Liu,² H. Chen,² X. H. Chen,² N. D. Zhigadlo,³ S. Katrych,³ Z. Bukowski,³ and J. Karpinski,³

¹National High Magnetic Field Laboratory, Florida State University, Tallahassee-FL 32310, USA

²Hefei National Laboratory for Physical Science a Microscale and Department of Physics, University of Science and Technology of China, Hefei, Anhui 230026, People's Republic of China and

³Laboratory for Solid State Physics, ETH Zürich, CH-8093 Zürich, Switzerland

(Dated: August 23, 2021)

To probe manifestations of multiband superconductivity in oxypnictides, we measured the angular dependence of magnetic torque $\tau(\theta)$ in the mixed state of $\text{SmO}_{0.8}\text{F}_{0.2}\text{FeAs}$ single crystals as functions of temperature T and high magnetic field H up to 30 T. We show that the effective mass anisotropy parameter γ extracted from $\tau(\theta)$, can be greatly overestimated if the strong paramagnetism of Sm or Fe ions is not properly taken into account. The correctly extracted γ depends on both T and H , saturating at $\gamma \simeq 9$ at lower temperatures. Neither the London penetration depth nor the superfluid density is affected by high fields up to the upper critical field. Our results indicate two strongly-coupled superconducting gaps of nearly equal magnitudes.

PACS numbers: 74.25.-q, 74.25.Ha, 74.25.Op, 74.70.Dd

The recently discovered superconducting oxypnictides [1, 2] have similarities with the high T_c cuprates, such as the emergence of superconductivity upon doping a parent antiferromagnetic compound [2, 3, 4]. Several theoretical models [5, 6] suggest unconventional superconducting pairing, while the Andreev spectroscopy [7], penetration depth [8], and photoemission measurements [9] indicate nodless s-wave pairing symmetry. Experiments [9, 10, 11] have found evidence for multi-gap superconductivity, in agreement with theoretical predictions [5].

The comparatively high T_c values and extremely high upper critical fields H_{c2} of the oxypnictides [10, 12] indicate promising prospects for technological applications if, unlike the layered cuprates, a sizeable vortex liquid region responsible for dissipative flux flow does not dominate their temperature-magnetic field ($T - H$) phase diagram. It is therefore important to reveal the true behavior of the anisotropic magnetization in the vortex state of the oxypnictides, particularly the extent to which vortex properties are affected by strong magnetic correlations, multiband effects and possible interband phase shift between the order parameters on different pieces of the Fermi surface [5]. For instance, multiband effects in MgB_2 can manifest themselves in strong temperature and field dependencies for the mass anisotropy parameter $\gamma(T, H)$ and the London penetration depth $\lambda(T, H)$ even at $H \ll H_{c2}$ [13, 14]. Yet, there are significant differences between two-band superconductivity in MgB_2 and in oxypnictides: in MgB_2 the interband coupling is weak, while in the oxypnictides it is the strong interband coupling which is expected to result in the high T_c [5]. Thus, probing multiband superconductivity in oxypnictides by magnetization measurements requires high magnetic fields, which can suppress the superfluid density in the band with the largest coherence length above the

“virtual upper critical field” (H_v) at which the vortex cores in this band overlap. In this Letter we address these issues, presenting the first high-field torque measurements of anisotropic reversible magnetization of the vortex lattice in $\text{SmO}_{0.8}\text{F}_{0.2}\text{FeAs}$ single crystals. Our measurements of $\gamma(T, H)$ up to 30T and extended temperature range, $20 < T < 40$ K have revealed a different behavior of $\gamma(T, H)$ as compared to recent low-field torque measurements [11].

Measurements of anisotropic equilibrium magnetization $m(T, H)$ in $\text{SmO}_{0.8}\text{F}_{0.2}\text{FeAs}$ are complicated by the smallness of $m(H, T)$ caused by the large Ginzburg-Landau parameter, $\kappa = \lambda/\xi > 100$ and by the strong paramagnetism of Sm^{3+} ions, which can mask the true behavior of $m(T, H)$. In this situation torque magnetometry is the most sensitive technique to measure the fundamental anisotropy parameters of $\mathbf{m}(\mathbf{T}, \mathbf{H})$ in small single crystals. The torque $\tau = \mathbf{m} \times \mathbf{H}$ acting upon a uniaxial superconductor is given by

$$\tau(\theta) = \frac{HV\phi_0(\gamma^2 - 1)\sin 2\theta}{16\pi\mu_0\lambda_{ab}^2\gamma\varepsilon(\theta)} \ln \left[\frac{\eta H_{c2}^{ab}}{\varepsilon(\theta)H} \right] + \tau_m \sin 2\theta, \quad (1)$$

where V is the sample volume, ϕ_0 is the flux quantum, H_{c2}^{ab} is the upper critical field along the ab planes, $\eta \sim 1$ accounts for the structure of the vortex core, θ is the angle between \mathbf{H} and the c-axis, $\varepsilon(\theta) = (\sin^2 \theta + \gamma^2 \cos^2 \theta)^{1/2}$ and $\gamma = \lambda_c/\lambda_{ab}$ is the ratio of the London penetration depths along the c-axis and the ab-plane. The first term in Eq. (1) was derived by Kogan in the London approximation valid at $H_{c1} \ll H \ll H_{c2}$ [15]. The last term in Eq. (1) describes the torque due to paramagnetism of the SmO layers and possible intrinsic magnetism of the FeAs layers. Here $\tau_m = (\chi_c - \chi_a)VH^2/2$ and χ_c and χ_a are the normal state magnetic susceptibilities of a uniaxial crystal along the c-axis and ab plane,

respectively. As will be shown below, the paramagnetic term in Eq. (1) in $\text{SmO}_{0.8}\text{F}_{0.2}\text{FeAs}$ can be larger than the superconducting torque, which makes extraction of the equilibrium vortex magnetization rather nontrivial. In this Letter we develop a method, which enables us to resolve this problem and measure the true angular dependence of the superconducting torque as a function of both field and temperature, probing the concomitant behavior of $\gamma(T, H)$ and $\lambda_{ab}(T, H)$ and manifestations of multiband effects in $\text{SmO}_{0.8}\text{F}_{0.2}\text{FeAs}$ single crystals.

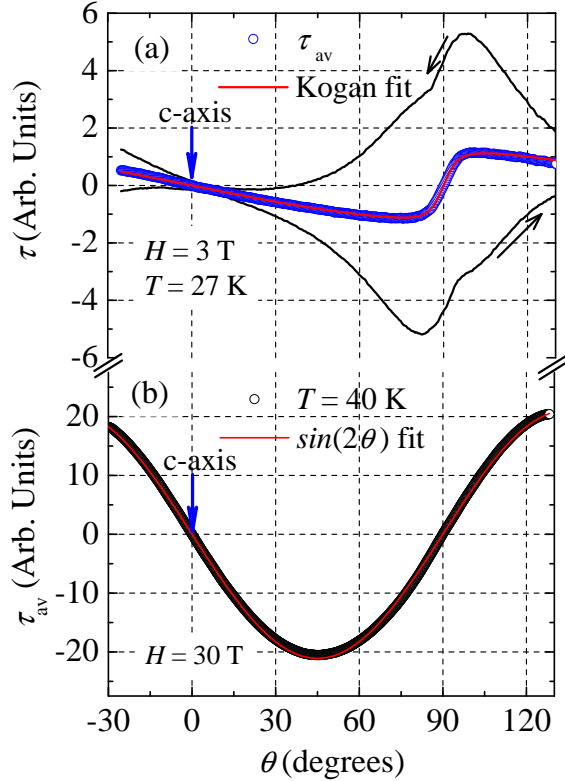


FIG. 1: (color online) (a) Magnetic torque $\tau(\theta)$ for a $\text{SmO}_{0.8}\text{F}_{0.2}\text{FeAs}$ single crystal for increasing and decreasing angle sweeps (black lines) at 3 T and 27 K. The equilibrium $\tau_{av}(\theta)$ (blue markers) is obtained by averaging both traces. (b) $\tau_{av}(\theta)$ for 40 K and 30T exhibits a nearly sinusoidal angular dependence. Red line corresponds to a fit to the first term in Eq. (1) with $\gamma = 11.5$.

Underdoped single crystals of $\text{SmO}_{1-x}\text{F}_x\text{FeAs}$ having typical sizes, $100 \times 100 \times 10 \mu\text{m}^3$ and $T_c \simeq 45\text{K}$ were grown by the flux method described in Ref. [16]. The sample was attached to the tip of a piezo-resistive micro-cantilever placed into a rotator inserted into a vacuum can. The ensemble was placed into a ^4He cryostat coupled to a resistive 35 T dc magnet of the National High Magnetic Field Lab. Changes in the resistance of the micro-cantilever associated with its deflection and thus a finite magnetic torque τ was measured via a Wheatstone resistance bridge.

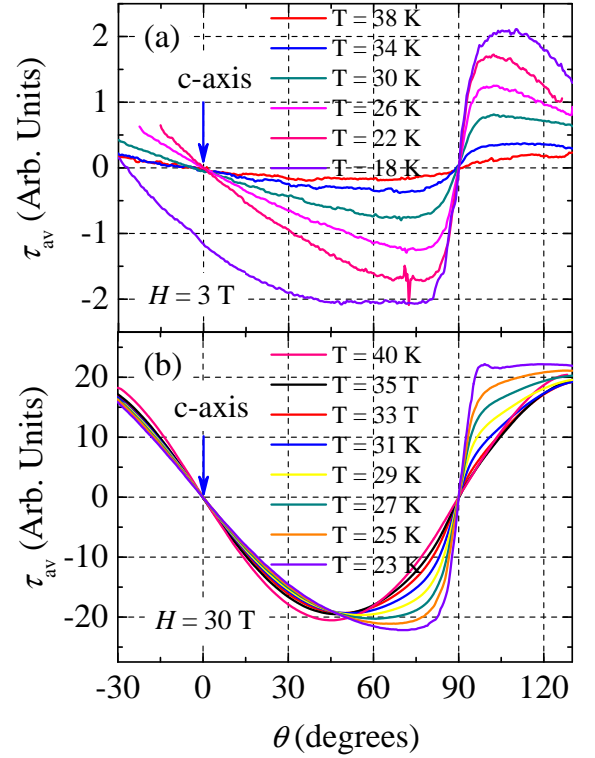


FIG. 2: (color online) (a) Angular dependence of $\tau_{av}(\theta)$ at 3 T and several temperatures. (b) Same as in (a) for 30 T.

Fig. 1 (a) shows typical angular dependence of $\tau(\theta)$ at 27 K and 3 T. Since we are only interested in temperature and field dependencies of γ and λ , the torque data are provided in arbitrary units. A hysteresis, resulting from the irreversible magnetization is observed between increasing and decreasing angle sweeps. Black markers depict the average value of both traces, $\tau_{av}(\theta) = (\tau_{\uparrow}(\theta) + \tau_{\downarrow}(\theta))/2$ defined as an equilibrium magnetization, where the arrows indicate increasing or decreasing angle sweeps. The red line is a fit to the first term in Eq. (1) with $\gamma \approx 11.5$ a value that is $\simeq 25\%$ smaller than the value reported in Ref. [11]. However, this multiparameter fit is not very suitable for extraction of the true values of γ due to pronounced error bars for H_{c2}^{ab} and a significant paramagnetic component particularly at 30T. The complete set of the raw $\tau_{av}(\theta)$ data is shown in Figs. 2 (a) and (b).

The superconducting component of the torque can be unambiguously extracted from the data by fitting the sum of two measured curves $\tau_{av}(\theta) + \tau_{av}(\theta + 90^\circ)$, in which the paramagnetic component cancels out:

$$\tau(\theta) + \tau(\theta + 90^\circ) = \frac{V\phi_0(\gamma^2 - 1)H \sin 2\theta}{16\pi\mu_0\lambda_{ab}^2\gamma} \times \left[\frac{1}{\varepsilon(\theta)} \ln \left(\frac{\eta H_{c2}^{ab}}{\varepsilon(\theta)H} \right) - \frac{1}{\varepsilon^*(\theta)} \ln \left(\frac{\eta H_{c2}^{ab}}{\varepsilon^*(\theta)H} \right) \right], \quad (2)$$

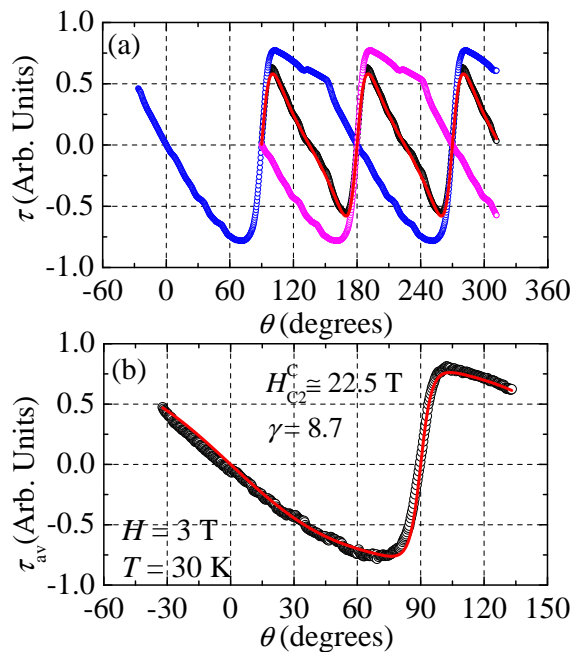


FIG. 3: (color online) Angular dependence of $\tau_{av}(\theta)$ (blue) and $\tau_{av}(\theta + 90^\circ)$ (magenta) for 3 T and 30 K. Red line corresponds to a fit of $\tau_{av}(\theta) + \tau_{av}(\theta + 90^\circ)$ to Eq. (2). (b) An example of the fit of $\tau_{av}(\theta)$ to Eq. (1) with the parameters taken from Fig. 3 (a).

where $\varepsilon^*(\theta) = (\cos^2 \theta + \gamma^2 \sin^2 \theta)^{1/2}$. This procedure is illustrated by Fig. 3 (a) where $\tau_{av}(\theta)$ for 3T and 30K is plotted together with $\tau_{av}(\theta + 90^\circ)$. Black markers depict the sum of both traces which is entirely determined by the superconducting response. Red line corresponds to a fit to Eq. (2), where $\eta H_{c2}^{ab}[T] \approx 315(1 - T^2/T_c^2)$ shown in the inset of Fig. 4 was extracted from the onset of the resistive transition in polycrystalline $\text{SmO}_{0.8}\text{F}_{0.2}\text{FeAs}$ with $T_c \simeq 47\text{K}$ [12]. The onset of the resistive transition reflects the behavior of those crystallites having the field along the ab-plane thus $H_{c2}^a(T)$. Given the lack of high-field $H_{c2}(T)$ data for our single crystals, the use of the measured value H_{c2}^{ab} for polycrystals eliminates the ambiguities of the multiparameter fit if H_{c2} in Eq. (2) is treated as one more fit parameter. Using the superconducting parameters obtained by this method in Eq. (1) we then fit the original $\tau_{av}(\theta)$ (red line in Fig. 3 (b)), treating τ_m as the only adjustable parameter. This method does result in an excellent fit, allowing us to extract both the superconducting torque and the paramagnetic torque associated with Sm or Fe moments. It also gives smaller values for $\gamma(T)$ than the ones obtained by direct fitting $\tau_{av}(\theta)$ uniquely to the first term of Eq. (1). As shown in Figs. 4 and 5 (a), the so-obtained γ is not only temperature dependent [11] but it is also field dependent, decreasing by more than 20 % at 30 T.

The obtained temperature dependence of $\gamma(T, H)$ is reminiscent of the behavior of $\gamma(T, H)$ previously re-

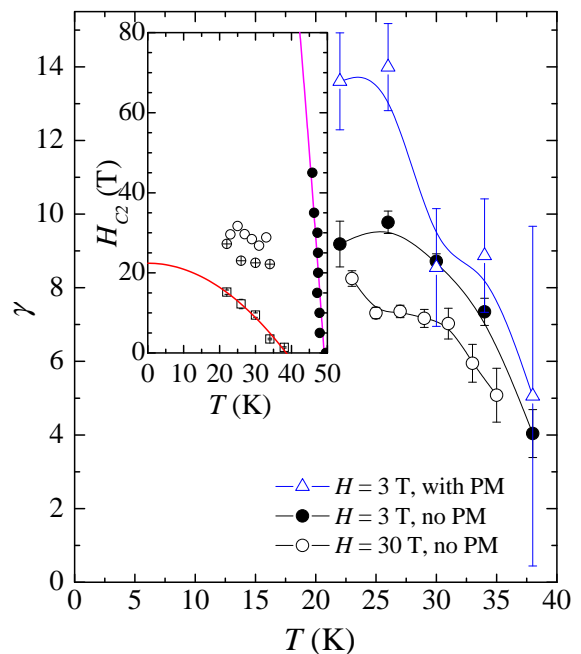


FIG. 4: (color online) Temperature dependencies of γ obtained from fitting $\tau_{av}(\theta) + \tau_{av}(\theta + 90^\circ)$ to Eq. (2) for 3T (solid circles) and 30T (open circles). The ambiguity of the extraction of γ from a direct multiparameter fit of $\tau_{av}(\theta)$ [11] to the first term in Eq. (1) is illustrated by the triangles. Inset shows the difference of H_{c2} for different fit procedures. Squares correspond to ηH_{c2}^c obtained by fitting the raw $\tau_{av}(\theta, T, H = 3\text{T})$ solely to first term in Eq. (1). Solid circles correspond to H_{c2}^c measured on a polycrystalline $\text{SmO}_{0.8}\text{F}_{0.2}\text{FeAs}$ with a $T_c \sim 47\text{K}$ [12] which we used to fit the data to Eq. (2) and from which we obtain $H_{c2}^c = H_{c2}^{ab}/\gamma$ (open circles are points from $H = 3\text{T}$ while crossed circles from $H = 30\text{T}$).

ported for MgB_2 which was explained in terms of multi-band effects [13, 14]. Yet the extracted London penetration depth shown in Fig. 5 (a) does not exhibit a significant field dependence which would indicate an abrupt depression of the superfluid density in one of the bands above H_v (produced by the suppression of the respective superconducting gap). This is quite remarkable given that we measured $\lambda(T, H)$ up to the applicability limit of the London theory, i.e. $\eta H_{c2}^c/H \simeq 1$ at $H = 30\text{T}$. Overall, the behaviors of $\gamma(T, H)$ and $\lambda(T, H)$ shown in Fig. 5 (a) would suggest two strongly coupled gaps of similar magnitude but not too different mass anisotropies. The decrease of $\gamma(H)$ as H increases may indicate that the band with the shorter coherence length $\xi \sim \hbar v_F/\Delta$ is the least anisotropic.

The relative contributions of the superconducting and magnetic components in $\tau_{av}(\theta, T, H)$ are shown in Fig. 5 (b). At higher T the behavior of $\tau_m(T) \propto C_1/T[K] + C_2$, $C_2 \approx -C_1/43$ at 3T is consistent with the Curie-Weiss paramagnetism of Sm^{3+} ions. However, this temperature dependence of $\tau_m(T)$ changes at $H = 30\text{T}$, for

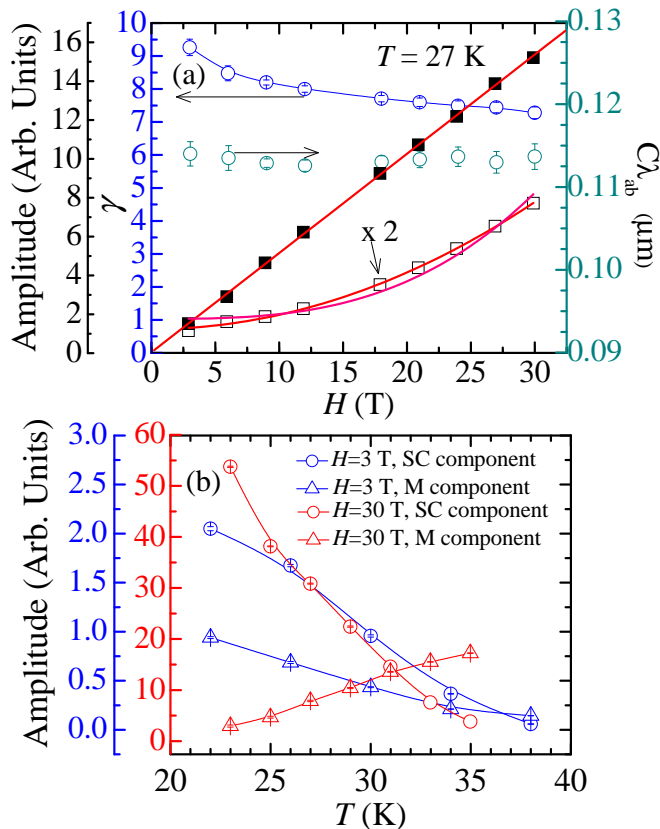


FIG. 5: (color online) (a) Field dependence of γ (blue markers) and $C\lambda_{ab}$ (green markers) obtained by fitting $(\tau(\theta) + \tau(\theta + 90^\circ))$ at $T = 27$ K to Eq. (2). Here, C is a calibration dependent constant for our cantilever. Black markers depict the field dependence of respectively the magnetic (open squares) and superconducting (solid squares) components. For clarity the data was multiplied by a factor of two. Red line corresponds to a T^2 fit and the magenta line to a T^3 dependence. (b) Amplitudes of superconducting (circles) and magnetic (triangles) components of $\tau_{av}(\theta)$, at $H = 3$ T (blue markers) and 30 T (red markers).

which $\tau_m(T)$ decreases as T decreases, indicating the intriguing possibility of field-induced antiferromagnetism (AF). Indeed, the coexistence of AF and superconductivity in phase-separated regions has been reported in the oxyphnictides [17], while AF in the vortex cores of the cuprates has been observed at higher field [18]. In our case, the latter can be ruled out since the observed $\tau_m(H, T = 27\text{K})$ follows a H^2 dependence, unlike $\tau_m \propto H^3/H_{c2}$ for the AF cores. Another mechanism may result from a field-dependent uniaxial magnetic anisotropy as the Sm^{3+} moments align along the field. This effect can be modeled by the single-ion Hamiltonian $\hat{H} = \mu_B(g_a\sigma_x H_x + g_a\sigma_y H_y + g_c\sigma_z H_z)/2$, where σ_α are the Pauli matrices, and g_α are the principal values of the effective g -factor tensor [19]. In this case

$$\tau_p = n\mu_B(g_c^2 - g_a^2)H \sin 2\theta \tanh(\mu_B g_\theta H / 2T) / 2g_\theta, \quad (3)$$

where n is the density of paramagnetic ions, $g_\theta = (g_c^2 \cos^2 \theta + g_a^2 \sin^2 \theta)^{1/2}$. For weak fields or $\mu_B g_\theta H \ll T$, Eq. (3) gives $\tau_p = (\chi_c - \chi_a)H^2 \sin 2\theta / 2$ and $\chi_\alpha = \mu_B^2 g_\alpha^2 / 4T$ as used in our analysis. However, for higher fields $\mu_B g_\theta H > T$, the paramagnetic torque $\tau_p \simeq n\mu_B(g_c^2 - g_a^2)H \sin 2\theta / 2g_\theta$ acquires higher order harmonics. This case may pertain to our data at 30 T and $T < 30$ K, for which the pure $\sin 2\theta$ component in $\tau(\theta)$ does decrease as T decreases, but $\tau_p(\theta)$ may not be completely eliminated by the procedure described above. Deviations from Eq. (1) also come from corrections to the London theory at high fields resulting in additional terms $\propto \alpha H_{c2}/H - (\ln \eta + \alpha)H/H_{c2}$, $\alpha \sim 1$ in $\mathbf{m}(T, H, \theta)$ due to pairbreaking and nonlocal effects [20].

In summary, our torque measurements at high-fields reveal the temperature and field dependencies of the anisotropic reversible magnetization which is strongly coupled with the magnetism of rare earth ions in $\text{SmO}_{0.8}\text{F}_{0.2}\text{FeAs}$ single crystals. Our results indicate a temperature and field dependent mass anisotropy $\gamma(T, H)$ which saturates at $\gamma \simeq 9$ at low temperatures under a modest field. This value is higher than $\gamma = H_{c2}^c/H_{c2}^a \simeq 5$ at low temperatures in $\text{NdO}_{0.7}\text{F}_{0.3}\text{FeAs}$ single crystals [21] and $\gamma \simeq 5 - 7$ for $\text{YBa}_2\text{Cu}_3\text{O}_{7-\delta}$, but is much smaller than $\gamma \geq 30$ suggested by Ref. [22]. The observed insensitivity of the London penetration depth at fields up to 30 T is indicative of strong coupling superconductivity, which in addition to a not very high γ is very important for applications. Our results are consistent with strongly coupled gaps of nearly equal magnitudes in distinct bands.

The NHMFL is supported by NSF through NSF-DMR-0084173 and the State of Florida. This work was also supported by NHMFL/IHRP (LB, AG, DCL), NHMFL-Schuller program (YJJ) and by AFOSR (DCL and AG). Work in Zurich was supported by the Swiss National Science Foundation through the NCCR pool MaNEP.

-
- [1] Y. Kamihara *et al.* **130**, 3296 (2008); H. Takahashi *et al.*, Nature **453**, 376 (2008); X. H. Chen *et al.*, Nature **453**, 761 (2008).
 - [2] G. F. Chen *et al.* Phys. Rev. Lett. **100**, 247002 (2008).
 - [3] Y. Takabayashi *et al.*, J. Am. Chem. Soc. **130**, 9242 (2008).
 - [4] C. de la Cruz *et al.*, Nature **453**, 899 (2008).
 - [5] I. I. Mazin, D. J. Singh, M. D. Johannes, and M. H. Du, Phys. Rev. Lett. **101**, 057003 (2008).
 - [6] K. Haule, J. H. Shim, and G. Kotliar, Phys. Rev. Lett. **100**, 226402 (2008); Q. Si and E. Abrahams, Phys. Rev. Lett. **101**, 076401 (2008); P. A. Lee, X. G. Wen, arXiv:0804.1739 (2008).
 - [7] T. Y. Chen, Z. Tesanovic, R. H. Liu, X. H. Chen, and C. L. Chien, Nature **453**, 1224 (2008).
 - [8] L. Malone *et al.*, arXiv:0806.3908 (2008).
 - [9] H. Ding *et al.*, Europhys. Lett. **83**, 47001 (2008).

- [10] F. Hunte *et al.*, *Nature* **453**, 903 (2008).
- [11] S. Weyeneth *et al.*, arXiv:0806.1024v1 (2008)
- [12] Y. J. Jo, et al. (unpublished); J. Jaroszynski *et al.*, *Phys. Rev. B* **78**, 064511 (2008).
- [13] M. Angst *et al.*, *Phys. Rev. Lett.* **88**, 167004 (2002); A. V. Sologubenko *et al.* *Phys. Rev. B* **65**, 180505(R) (2002); S. L. Bud'ko and P. C. Canfield, *ibid.* **65** 212501 (2002)
- [14] R. Cubitt *et al.*, *Phys. Rev. Lett.* **91**, 047002, (2003); M. Angst *et al.*, *Phys. Rev. B* **70**, 224513 (2004).
- [15] V. G. Kogan, *Phys. Rev. B* **24**, 1572 (1981); *Phys. Rev. Lett.* **89**, 237005 (2002).
- [16] N. D. Zhigadlo, S. Katrych, Z. Bukowski, and J. Karpinski, *J. Phys.: Condens. Matter* **20**, 342202 (2008).
- [17] See, for example, T. Goko *et al.*, arXiv:0808.1425 (2008).
- [18] V. F. Mitrovic *et al.*, *Nature* **413**, 501 (2001); B. Lake *et al.*, *Nature* **415**, 299 (2002); H. J. Kang *et al.*, *Nature* **423**, 522 (2003).
- [19] R. M. White *Quantum Theory of Magnetism*, Springer-Verlag, Berlin, Heidelberg, New York, 1983.
- [20] V. G. Kogan *et al.*, *Phys. Rev. B* **74**, 184521 (2006).
- [21] J. Jaroszynski *et al.*, *Phys. Rev. B* **78**, 174523 (2008).
- [22] A. Dubroka *et al.*, *Phys. Rev. Lett.* **101**, 097011 (2008).